

Potential Phosphorylation Site Modulates The Dimerization and Activity of KIF1A*

LIU Bei^{1,2**}, YUE Yang^{2**}, YU Yong², REN Jin-Qi², FENG Wei^{2***}, HUO Lin^{2***}, XU Tao^{1,2***}

¹ College of Life Science and Technology, Huazhong University of Science and Technology, Wuhan 430074, China;

² National Laboratory of Biomacromolecules, Institute of Biophysics, Chinese Academy of Sciences, Beijing 100101, China)

Abstract Kinesin-3 KIF1A is responsible for the anterograde transport of synapse vesicle (SV) precursors in axons. The CC1-FHA tandem of KIF1A has been revealed as a stable dimer that can trigger motor activity, but the mechanism underlying the regulation of the CC1-FHA dimer is unclear. Based on the CC1-FHA dimer structure, we found a potential phosphorylation motif "487SPKK⁴⁹⁰" located at the dimer interface. We demonstrated that the phosphorylation-mimetic mutation of Ser487 leads to the dissociation of the CC1-FHA dimer. Moreover, the Ser487-mutation could regulate the motor activity of KIF1A and the KIF1A-mediated axonal transport activity of SVs in *C. elegans*. Thus, the highly conserved "487SPKK⁴⁹⁰" motif may be a key site in the CC1-FHA tandem for regulating CC1-FHA dimerization and the subsequent activity of KIF1A.

Key words KIF1A, phosphorylation, dimerization, axonal transport

DOI: 10.3724/SP.J.1206.2014.00073

Kinesin motors play prominent roles in transporting membranous organelles/vesicles, protein complexes and mRNA along the microtubule and in assembling the spindles during cell division^[1-2]. So far, 14 kinesin families have been identified. The mammalian KIF1A belongs to the kinesin-3 family, which is responsible for the fast anterograde transport of SV precursors in axon^[3-4].

Previous data revealed that, in the inactive state, the kinesin-1 motor exists in a folded compact conformation in solution. In most species, kinesin-1 is a heterotetramer that has two kinesin heavy chains (KHC) and two kinesin light chains (KLC). The C-terminal tail of KHC can fold and inhibit the motor domain by disrupting microtubule binding and ATPase activity^[5]. KLC can push KHC apart to keep it in an inactive status^[6]. In contrast, KIF1A has three discrete coiled-coil domains (CC1 to CC3) and a FHA domain in the middle. CC1-FHA-CC2 can regulate the dimerization and activity of KIF1A (Figure 1a). The CC2 domain can fold back to interact with the FHA domain and inhibit microtubule binding^[7]. The CC1 domain can inhibit the processive motility of KIF1A

by promoting its monomeric state^[8]. The CC1-FHA tandem can dimerize and activate KIF1A by preventing the exposure of the CC1 domain and a linker between the CC1 and FHA domains, both of which are essential for motor inhibition^[9].

Phosphorylation is a crucial factor in regulating the autoinhibition of kinesin motors. For the kinesin-5 family member KIF11, phosphorylation of the C-terminal tail by cyclin-dependent kinase 1 (CDK-1) can release the autoinhibition and increase microtubule binding^[10]. In contrast, Jun N-terminal kinase 3 (JNK3) can phosphorylate the motor domain of kinesin-1,

*This work was supported by grants from The National Basic Research Program of China (2010CB833701, 2011CB910503, 2014CB910202) and The National Natural Science Foundation of China (31130065, 31300611, 31190062, 31200577).

**These authors contributed equally to this work.

***Corresponding author.

XU Tao. Tel: 86-10-64888469, E-mail: xutao@ibp.ac.cn

HUO Lin. Tel: 86-10-64888853, E-mail: holly@moon.ibp.ac.cn

FENG Wei. Tel: 86-10-64888751, E-mail: wfeng@ibp.ac.cn

Received: March 17, 2014 Accepted: May 30, 2014

which can stabilize the autoinhibited conformation^[11]. Active glycogen synthase kinase 3 (GSK-3) can also inhibit the anterograde transport of kinesin-1^[12].

Based on the structure of the CC1-FHA dimer^[9], we find that there is a potential Pro-directed phosphorylation site "487SPKK⁴⁹⁰" in the CC1-FHA domain. In this study, we created a phosphorylation-mimetic mutation, S487D, in which an aspartic acid residue mimics the negative charge of phosphate; as a control, we generated alanine at the Ser487 site (S487A) to preclude phosphorylation. The S487D mutation introduced a phosphate group to the hydrophobic CC1-FHA dimer interface, thus causing the dimer to dissociate. In contrast, the S487A construct could form a more stable dimer than wild type. To investigate the effects of the phosphorylation of S487 on KIF1A-mediated axonal transport, we tested the localization and microtubule binding capability of KIF1A in mammalian cells and the localization of cargoes in the axon of DB motor neurons in *C. elegans*. We found that the two mutations S487A and S487D exhibited distinct behaviors with respect to their effects on the microtubule binding, localization and transport ability of SVs in the axon. The S487D mutation inhibited the microtubule binding of KIF1A, and the mutant accumulated mainly in the cell body. In contrast, the S487A mutant could bind to microtubules and appeared prominently at the end of neuronal tips. Furthermore, we demonstrated that the S487D mutant failed to transport SVs to the axon, whereas the S487A mutant succeeded. Our study indicated that phosphorylation might be crucial for KIF1A-mediated axonal transport.

1 Materials and methods

1.1 Plasmid construction, cell culture and transfection

A truncated KIF1A construct was PCR amplified from the full-length mouse KIF1A^[4] and cloned into vector pEGFP-N1. All mutants were generated using the standard PCR-based mutagenesis method. The COS-7 and HEK293 cells were cultured in DMEM with 10% fetal bovine serum (FBS). The N2A cells were cultured in DMEM/F12 (1 : 1) with 10% FBS. The cells were transfected with Lipofectamine 2000 according to the manufacturer's instructions (Invitrogen).

1.2 Chemical cross-linking assay

As in a typical cross-linking reaction, 20 μ g protein samples were mixed with freshly prepared disuccinimidylglutarate (DSG, from PIERCE) to a final concentration of 1.5 mmol/L. The mixture was incubated at room temperature for 10 min, and the reaction was quenched by the addition of excess amounts of 1 mol/L Tris-HCl stock solution. The samples were then checked using SDS-PAGE with Coomassie-blue staining.

For the *in vivo* cross-linking assay, HEK293 cells were transfected with Myc-tagged KIF1A WT fragments and the mutants were harvested for the reaction. The harvested cells were resuspended in PBS buffer and incubated with 2 mmol/L DSG for 45 min at room temperature. After reaction, the treated cells were centrifuged and then resuspended in lysis buffer (50 mmol/L Tris-HCl, pH 7.4, 150 mmol/L NaCl, 1 mmol/L EDTA, 1% TritonX-100) containing protease inhibitors for 30 min on ice. The cell lysates were analyzed using SDS-PAGE and Western blot using anti-Myc antibody (MBL).

1.3 *In vitro* kinase assay

In each kinase reaction, 10 μ l protein sample (50 μ mol/L) was mixed with 1 μ l purified active Cdk5/p25^[13]. The mixture was incubated at 30 °C for 1 h in the reaction buffer (50 mmol/L Tris-HCl, pH 8.0, containing 100 mmol/L NaCl, 2 mmol/L β -mercaptoethanol, 10 mmol/L MgCl₂, 2 μ Ci [γ -³²P]-ATP (Perkin Elmer) and 100 μ mol/L non-radioactive ATP). The kinase reaction was terminated by adding 5 \times SDS-PAGE loading buffer with boiling. Samples were subjected to SDS-PAGE (12.5%), followed by Coomassie-blue staining and autoradiography.

1.4 *In vivo* microtubule binding and cell localization

Microtubule binding and cell localization assays in live cells were performed as described. Fluorescence images were obtained using Olympus FV500 Laser Scanning Confocal Microscopy with a 60 \times (NA=1.40) oil objective. The confocal settings used for the image capture were held constant in the comparison experiments. Data analysis was conducted using IGOR Pro (Wavemetrics) or SigmaPlot (Systat) software. The results are presented as the mean value \pm SD of the indicated experiments ($n > 15$). Asterisks denote statistical significance compared to control, *** $P < 0.001$.

1.5 *C. elegans* transformation and imaging

mkif1a::gfp with various mutations were produced by PCR from pGW1-*mkif1a* plasmid^[4] and cloned into pD95.75 vector containing *Punc-104* promoter. Germline transformation was performed using a standard microinjection method^[14]. In this method, 80 mg/L plasmids were injected into *unc104(e1265); ceIs62[Punc-129:ANF::Venus, Punc-129:RFP::SNB-1, Ptx-3::RFP]* worms. Multiple transgenic lines for each transgene were examined for fluorescence expression. Fluorescence images were obtained using Olympus FV500 Laser Scanning Confocal Microscopy with a 60×(NA=1.40) oil objective.

2 Results

2.1 Mutation of the residue S487 disrupts the dimerization of the CC1-FHA tandem

In kinesin-3 KIF1A, the CC1-FHA-CC2 tandem

functions as a regulatory center for controlling the activation of KIF1A (Figure 1a). The covalently linked CC1-FHA tandem forms a stable dimer to promote the formation of a motor that is required for processive movement. According to the published crystal structure of C-CC1-FHA^[9], the FHA domain adopts eleven strands (from $\beta 1$ to $\beta 11$), and C-CC1 forms a short α -helical structure (α CC1). In the C-CC1-FHA dimer, the covalent linker between C-CC1 and FHA domain is folded and forms a β -finger structure containing two antiparallel β strands, β F1 and β F2. Sequence analysis of the CC1-FHA tandem reveals that the conserved β F2/ β F1-loop contains a potential proline-directed phosphorylation site "487SPKK490" (Figure 1b). Interestingly, based on the structure of KIF1A C-CC1-FHA, residue Ser487 is located at the interface of the CC1-FHA dimer, and its hydroxyl group is readily accessible for potential

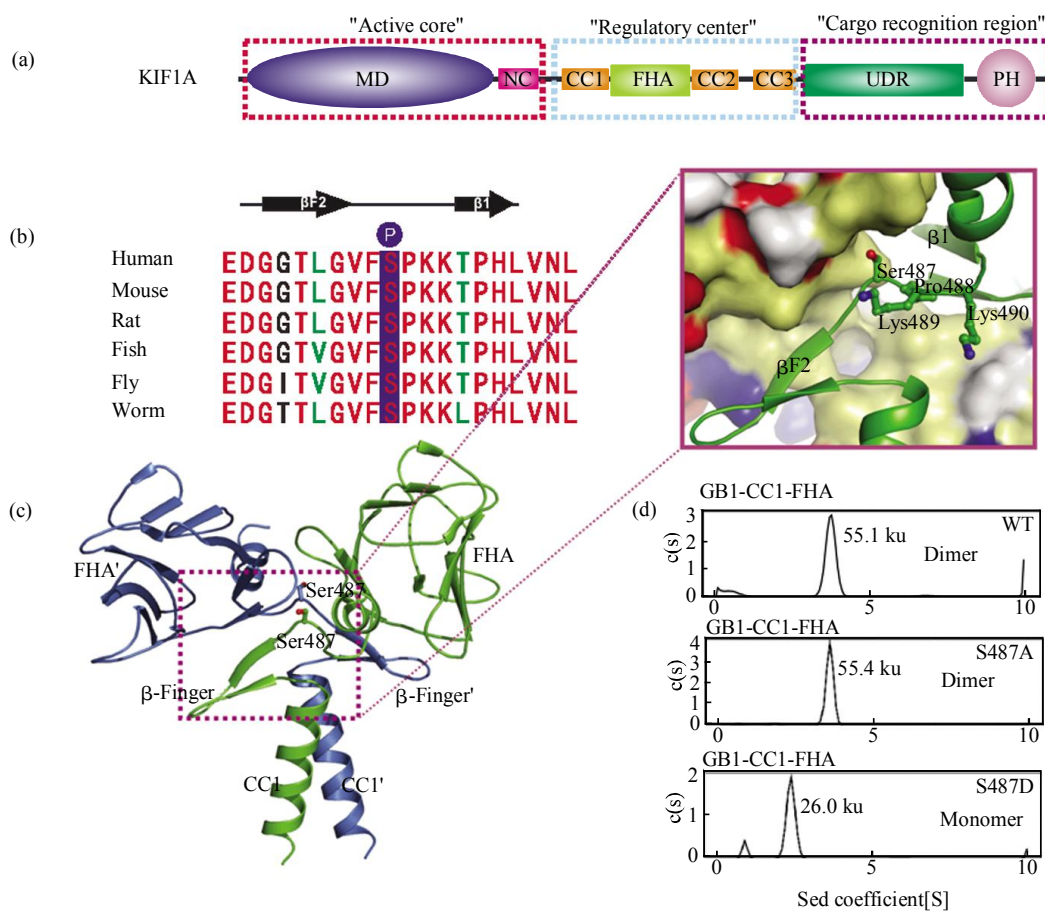


Fig. 1 The CC1-FHA dimer is convertible into a monomer by the phosphorylation-mimetic mutation at Ser487

(a) Schematic diagram of KIF1A. (b) Sequence alignment of KIF1A β F2/ β F1-loop revealed the conserved putative phosphorylation "487SPKK490"-motif. (c) Structure analysis of KIF1A C-CC1-FHA. S487 locates at the dimer interface and is surrounded by some hydrophobic residues. (d) Sedimentation velocity-based assays demonstrating that the Ser487 phosphorylation-mimetic mutation disrupts the CC1-FHA-mediated dimerization. Compared with the wild type (upper panel), S487A-CC1-FHA remained as a stable dimer (middle panel), whereas S487D-CC1-FHA became a stable monomer (lower panel).

phosphorylation (Figure 1c). We envisioned that the phosphorylation of Ser487 would introduce a bulky, negatively charged phosphate group into the hydrophobic CC1-FHA dimer interface, thus causing the dimer to dissociate. To test the above hypothesis, we substituted Ser487 with an aspartic acid. As control, Ser487 is replaced by an alanine. In agreement with previous data, the wild type CC1-FHA existed in a dimeric form, while the phospho-mimetic mutant S487D-CC1-FHA behaved as a monomer in the sedimentation velocity experiments. As for the control, the S487A-CC1-FHA mutant adopted a dimeric form in solution (Figure 1d). Taken together, these results indicate that the introduction of negative charge at residue 487 could disrupt CC1-FHA tandem dimerization.

2.2 Altering the S487 site affects the activity of KIF1A

Next, we created a version of KIF1A (KIF1A

(1~681)) truncated to the CC2 domain (the MNCFC fragment). A previous study indicated that this fragment remains autoinhibited, similar to the full-length KIF1A [8]. We checked the microtubule binding ability and cellular localizations of the MNCFC fragment. The nonhydrolyzable ATP analog AMPPNP (5'-adenylyl-beta, gamma-imidodiphosphate) can block the release of the active motor protein from microtubules [8]. In live cells, upon treatment with AMPPNP, WT-MNCFC and S487D-MNCFC did not become trapped in the microtubule but instead remained diffused in the cytosol (Figure 2a, b). Meantime, S487D-MNCFC showed more prominent localizations in cell body than WT-MNCFC (Figure 2c, d). These results indicate that the S487D mutant leads to the dissociation of the CC1-FHA dimer to keep the motor in an inactive status. In contrast, the S487A-MNCFC showed strong microtubule binding upon treatment with AMPPNP and increased

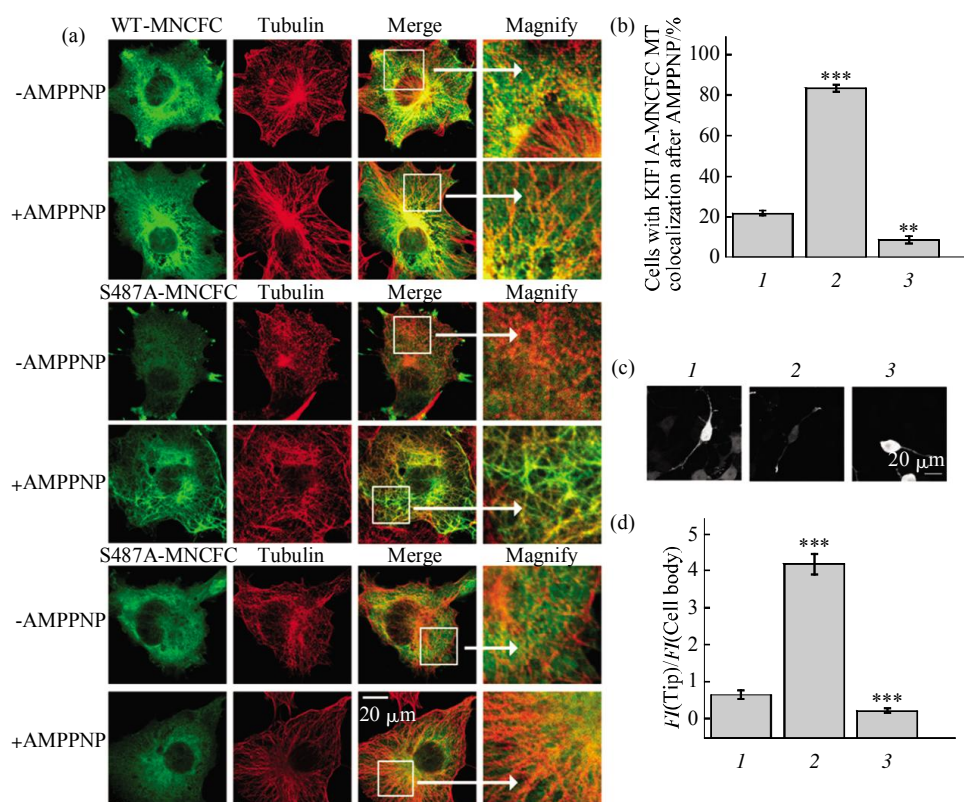


Fig. 2 Phosphorylation-mimetic of S487 site in the CC1-FHA tandem inhibits the activity of KIF1A

(a) *In vivo* microtubule binding assay of WT-MNCFC and its various mutants in COS-7 cells. Only S487A-MNCFC showed obvious microtubule binding capacity after treatment with AMPPNP. Neither WT-MNCFC nor S487D-MNCFC could bind with microtubule after treatment with AMPPNP. (b) Quantification of KIF1A-MNCFC colocalizations with microtubule after being treated with AMPPNP. (c) Cellular localizations of the WT-MNCFC and its various mutants in N2A cells. Compared with WT-MNCFC, S487D-MNCFC showed even more prominent localization in the cell body; S487A-MNCFC had a dramatically increased localization at cellular peripheries. (d) Quantification of the cellular distribution data showed in panel (c). The ratio of the tip to cell body fluorescence intensity (FI) was quantified for each construct for at least 20 cells ($n \geq 20$). The error is defined as the mean (\pm SEM), *** $P < 0.001$. 1: WT-MNCFC; 2: S487A-MNCFC; 3: S487D-MNCFC.

localizations at the end of neuronal tips (Figure 2), possibly due to the stabilization of the CC1-FHA dimer induced by the mutation.

Next, we tested the KIF1A-mediated axonal transport of SVs in *C. elegans*^[15-17]. Compared with the wild type control, the *unc-104* (*e1265*) allele with the loss of function of UNC-104 abolished the axonal transport of SNB-1-RFP-labeled SVs from the cell body to axons (Figure 3a). We detected axonal transport ability under the *unc-129* promoter, which can drive gene expression in the DA/DB motor neurons. Microinjection of the WT full-length KIF1A largely rescued, by up to 60%, the axonal transport defects caused by the UNC-104 mutation (Figure 3b, c). The S487D mutant could not rescue the transport defect of the *unc-104* (*e1265*) allele. In contrast, the S487A-KIF1A mutant could rescue, by up to 90%, the UNC-104 mutation-induced axonal vesicle transport defects (Figure 3b, c), presumably due to the mutation-induced stabilization of the dimeric conformation of KIF1A mediated by the CC1-FHA tandem. The above

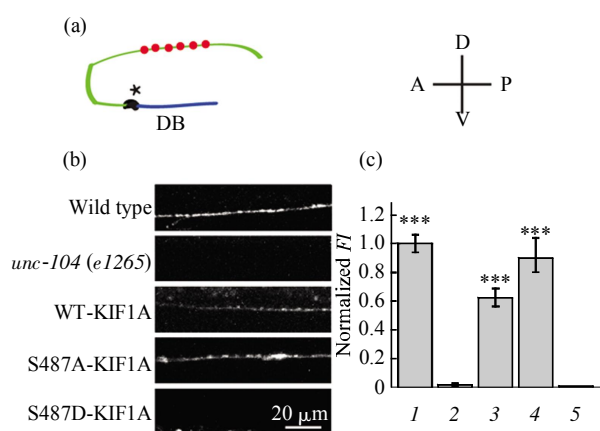


Fig. 3 Phosphorylation-mimetic of S487 site can regulate the KIF1A-mediated axon transport activity of SVs

(a) Schematic diagrams of DB motor neuron under the *unc-129* promoter used in this study. Dendrite is colored in blue. Axon is colored in green. The dotted region denotes the axon that was imaged and analyzed in (b) and (c). DB motor neurons process toward posterior. The processing directions shown are A: Anterior; D: Dorsal; P: Posterior; V: Ventral; an asterisk represents cell body. (b) KIF1A-mediated SNB-1-RFP-labeled SV transport in *C. elegans* motor neurons. The figure shows representative images of SNB-1-RFP fluorescence in axons of motor neurons from animals with the wild type, the *unc-104* (*e1265*) allele, the WT-KIF1A transgene, S487D-KIF1A transgene and S487A-KIF1A transgene. (c) Normalization of quantification of the SNB-1-RFP fluorescent intensity (FI) of axons in (b). Normalized FI is defined as the ratio of the fluorescent intensity of each transgene/allele to that of the wild type in axons. Error bars represent the standard error of the mean (\pm SEM), $n \geq 20$, *** $P < 0.001$. 1: Wild type; 2: *unc-104* (*e1265*); 3: WT-KIF1A; 4: S487A-KIF1A; 5: S487D-KIF1A.

in vivo data strongly indicate that the potential phosphorylation site of ¹⁴⁸⁷SPKK⁴⁹⁰ is essential for the KIF1A-mediated axonal transport activity.

2.3 The S487 site of KIF1A can be phosphorylated

To check whether the S487 site of the CC1-FHA tandem is a potentially phosphorylated site, we performed an *in vitro* phosphorylation assay using cyclin-dependent kinase-5 (CDK-5) and found that CC1-FHA can indeed be robustly phosphorylated (Figure S1 in **Supplementary material**). In contrast, the substitution of Ser487 with either Ala or Asp abolished the CDK-5-mediated phosphorylation of the CC1-FHA tandem (Figure S1 in **Supplementary material**).

3 Discussion

In this study, we found that the phospho-mimetic S487D-CC1-FHA mutant had a lower sedimentation coefficient than the wild-type protein. In contrast, the S487A-CC1-FHA mutant behaved as a dimer in solution. A similar result was also observed in the *in vivo* chemical cross-linking assay. Compared with the wild type, the S487D-MNCFC mutant showed a reduced cross-linked dimer, and the S487A-MNCFC mutant showed a robust cross-linked dimer, suggesting that a negatively charged residue at this position tends to form a monomer (Figure S2 in **Supplementary material**).

In our study with the truncated version of S487D-MNCFC, we found that the addition of a negative charge at the S487 site can lead KIF1A to dissociate from the microtubules. S487D-MNCFC distributes in the whole cytoplasm either before or after treatment with AMPPNP. Meanwhile, consistent with the cellular results, the mutant strain *unc-104* (*e1265*) expressed the WT-KIF1A, and S487A-KIF1A could mostly rescue the axonal SV transport defect. The strain *unc-104* (*e1265*) expressed the S487D-KIF1A and exhibited similar deficiency in the transport of SVs, accumulating in the cell body and thus indicating that the S487 phosphorylation-mimetic of KIF1A can result in the inhibition of axonal transport and can consequently affect signal transmitter release. We propose a model in which the Ser487 phosphorylation directs transport in the axon by dissociating the CC1-FHA dimer to inhibit the activity. Finally, although we did not know which kinase plays a role in phosphorylating the Ser487 of KIF1A, we showed that KIF1A can be phosphorylated by the Pro-directed

kinase CDK-5. There may be other kinases that can mediate the KIF1A phosphorylation. We conclude that the potential phosphorylation site of KIF1A can modulate the activity of KIF1A and may help further investigations of the kinase-mediated regulation of KIF1A.

Supplementary material Figure S1 and Figure S2 are available at PIBB website(<http://www.pibb.ac.cn>)

References

- [1] Vale R D. The molecular motor toolbox for intracellular transport. *Cell*, 2003, **112**(4): 467–480
- [2] Hirokawa N, Nitta R, Okada Y. The mechanisms of kinesin motor motility: lessons from the monomeric motor KIF1A. *Nat Rev Mol Cell Biol*, 2009, **10**(12): 877–884
- [3] Huckaba T M, Gennerich A, Wilhelm J E, *et al.* Kinesin-73 is a processive motor that localizes to Rab5-containing organelles. *J Biol Chem*, 2011, **286**(9): 7457–7467
- [4] Lee J R, Shin H, Ko J, *et al.* Characterization of the movement of the kinesin motor KIF1A in living cultured neurons. *J Biol Chem*, 2003, **278** (4): 2624–2629
- [5] Verhey K J, Rapoport T A. Kinesin carries the signal. *Trends in Biochemical Sciences*, 2001, **26** (9): 545–549
- [6] Cai D, Hoppe A D, Swanson J A, *et al.* Kinesin-1 structural organization and conformational changes revealed by FRET stoichiometry in live cells. *J Cell Biol*, 2007, **176** (1): 51–63
- [7] Lee J R, Shin H, Choi J, *et al.* An intramolecular interaction between the FHA domain and a coiled coil negatively regulates the kinesin motor KIF1A. *The EMBO Journal*, 2004, **23** (7): 1506–1515
- [8] Hammond J W, Cai D, Blasius T L, *et al.* Mammalian Kinesin-3 motors are dimeric *in vivo* and move by processive motility upon release of autoinhibition. *PLoS Biol*, 2009, **7** (3): e1000072
- [9] Huo L, Yue Y, Ren J, *et al.* The CC1-FHA tandem as a central hub for controlling the dimerization and activation of Kinesin-3 KIF1A. *Structure*, 2012, **20**(9): 1550–1561
- [10] Cahu J, Olichon A, Hentrich C, *et al.* Phosphorylation by Cdk1 increases the binding of Eg5 to microtubules *in vitro* and in *Xenopus* egg extract spindles. *PLoS One*, 2008, **3** (12): e3936
- [11] DeBerg H A, Blehm B H, Sheung J, *et al.* Motor domain phosphorylation modulates kinesin-1 transport. *J Biol Chem*, 2013, **288** (45): 32612–32621
- [12] Morfini G, Szebenyi G, Elluru R, *et al.* Glycogen synthase kinase 3 phosphorylates kinesin light chains and negatively regulates kinesin-based motility. *The EMBO Journal*, 2002, **21** (3): 281–293
- [13] Amin N D, Albers W, Pant H C. Cyclin-dependent kinase 5 (cdk5) activation requires interaction with three domains of p35. *J Neurosci Res*, 2002, **67**(3): 354–362
- [14] Mello C C, Kramer J M, Stinchcomb D, *et al.* Efficient gene transfer in *C. elegans*: extrachromosomal maintenance and integration of transforming sequences. *The EMBO Journal*, 1991, **10** (12): 3959–3970
- [15] Klopfenstein D R, Vale R D. The lipid binding pleckstrin homology domain in UNC-104 kinesin is necessary for synaptic vesicle transport in *Caenorhabditis elegans*. *Mol Biol Cell*, 2004, **15** (8): 3729–3739
- [16] Hall D H, Hedgecock E M. Kinesin-related gene *unc-104* is required for axonal transport of synaptic vesicles in *C. elegans*. *Cell*, 1991, **65** (5): 837–847
- [17] Yue Y, Sheng Y, Zhang H N, *et al.* The CC1-FHA dimer is essential for KIF1A-mediated axonal transport of synaptic vesicles in *C. elegans*. *Biochem Biophys Res Commun*, 2013, **435** (3): 441–446

调控 KIF1A 二聚化和活性的潜在的磷酸化位点 *

刘 贝^{1, 2)**} 岳 旻^{2)**} 俞 勇²⁾ 任锦启²⁾ 冯 巍^{2)***} 霍 麟^{2)***} 徐 涛^{1, 2)***}

(¹⁾ 华中科技大学生命科学与技术学院, 武汉 430074; (²⁾ 中国科学院生物物理研究所, 生物大分子国家重点实验室, 北京 100101)

摘要 驱动蛋白 kinesin-3 家族中的 KIF1A 蛋白主要参与轴突上分泌囊泡前体的正向运输. KIF1A 中的 CC1-FHA 片段能够形成稳定的二聚体结构, 同时促进驱动蛋白的活性, 但是其具体的调节机制尚未清楚. 基于已有的 CC1-FHA 二聚体的晶体结构, 我们发现在二聚体表面的“⁴⁸⁷SPKK⁴⁹⁰”位置存在潜在的磷酸化位点. 证明了将 487 位点模拟磷酸化后将导致 CC1-FHA 二聚体的解聚. 进一步, 在 487 位点进行点突变将影响 KIF1A 的活性以及线虫中 KIF1A 介导的突触囊泡在轴突上的运输. 因此, 高度保守的“⁴⁸⁷SPKK⁴⁹⁰”可能对 CC1-FHA 片段二聚化和调节 KIF1A 活性起着关键性作用.

关键词 KIF1A, 磷酸化, 二聚化, 轴突运输

学科分类号 Q71

DOI: 10.3724/SP.J.1206.2014.00073

* 国家重点基础研究发展计划(2010CB833701, 2011CB910503, 2014CB910202)和国家自然科学基金(31130065, 31300611, 31190062, 31200577)资助项目.

** 共同第一作者.

*** 通讯联系人.

徐 涛. Tel: 010-64888469, E-mail: xutao@ibp.ac.cn

霍 麟. Tel: 010-64888853, E-mail: holly@moon.ibp.ac.cn

冯 巍. Tel: 010-64888751, E-mail: wfeng@ibp.ac.cn

收稿日期: 2014-03-17, 接受日期: 2014-05-30

Supplementary material

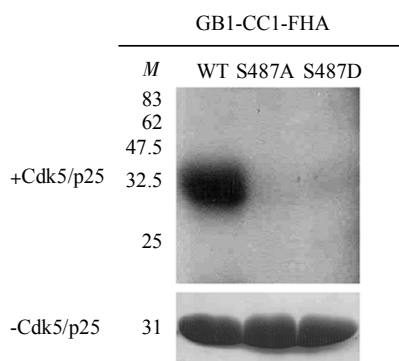


Figure S1 *In vitro* CDK-5 phosphorylation assay of the CC1-FHA tandem

The wild type protein showed a robust CDK-5-mediated phosphorylation. In contrast, neither S487A-CC1-FHA nor S487D-CC1-FHA showed detectable phosphorylation by CDK-5.

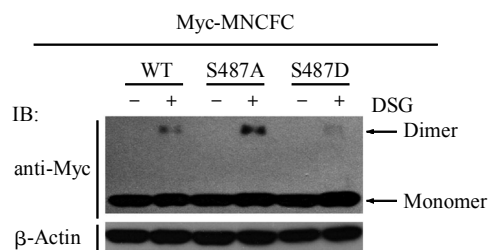


Figure S2 *In vivo* chemical cross-linking assay showing that S487D-mediated dissociation of the CC1-FHA dimer largely impaired the dimerization capacity of MNCFC, whereas S487A-induced stabilization of the dimer significantly enhanced the dimerization capacity.